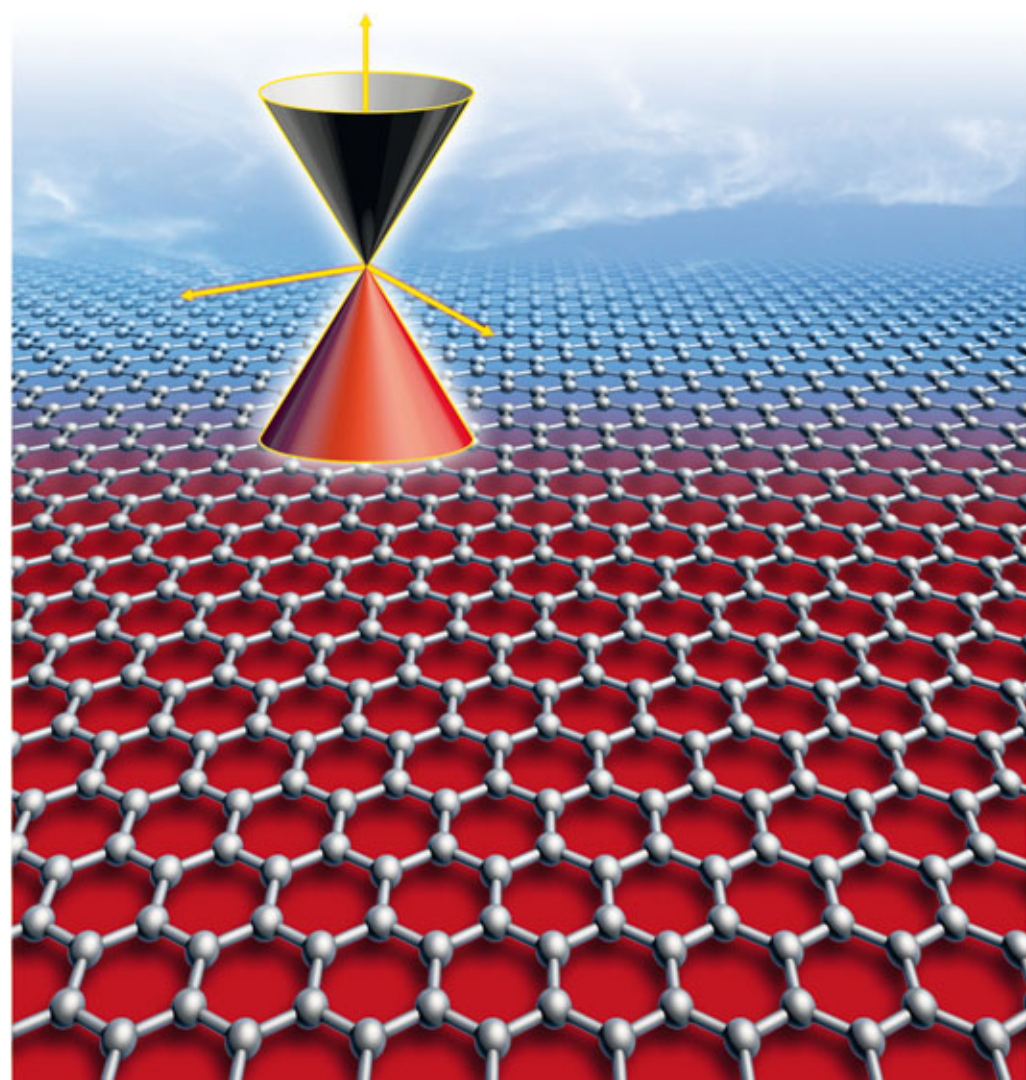


Edited by C. N. R. Rao and A. K. Sood

 WILEY-VCH

Graphene

Synthesis, Properties, and Phenomena



Edited by
C. N. R. Rao and A. K. Sood

Graphene

Related Titles

Martin, N., Nierengarten, J.-F. (eds.)

Supramolecular Chemistry of Fullerenes and Carbon Nanotubes

2012

ISBN: 978-3-527-32789-8

Saito, Y. (ed.)

Carbon Nanotube and Related Field Emitters

Fundamentals and Applications

2010

ISBN: 978-3-527-32734-8

Jorio, A., Dresselhaus, M. S., Saito, R., Dresselhaus, G.

Raman Spectroscopy in Graphene Related Systems

2011

ISBN: 978-3-527-40811-5

Krüger, A.

Carbon Materials and Nanotechnology

2010

ISBN: 978-3-527-31803-2

Kumar, C. S. S. R. (ed.)

Carbon Nanomaterials

Series: Nanomaterials for the Life Sciences (Volume 9)

2011

ISBN: 978-3-527-32169-8

Guldi, D. M., Martín, N. (eds.)

Carbon Nanotubes and Related Structures

Synthesis, Characterization, Functionalization, and Applications

2010

ISBN: 978-3-527-32406-4

Edited by C. N. R. Rao and A. K. Sood

Graphene

Synthesis, Properties, and Phenomena



**WILEY-
VCH**

WILEY-VCH Verlag GmbH & Co. KGaA

The Editors

Prof. Dr. C. N. R. Rao

Chemistry of Materials Unit
Jawaharlal Nehru Centre
Jakkur P.O.
Bangalore 560 064
India

Prof. Dr. A. K. Sood

Indian Institute of Science
Department of Physics
Bangalore 560 012
India

■ All books published by **Wiley-VCH** are carefully produced. Nevertheless, authors, editors, and publisher do not warrant the information contained in these books, including this book, to be free of errors. Readers are advised to keep in mind that statements, data, illustrations, procedural details or other items may inadvertently be inaccurate.

Library of Congress Card No.: applied for

British Library Cataloguing-in-Publication Data

A catalogue record for this book is available from the British Library.

Bibliographic information published by the Deutsche Nationalbibliothek

The Deutsche Nationalbibliothek lists this publication in the Deutsche Nationalbibliografie; detailed bibliographic data are available on the Internet at <<http://dnb.d-nb.de>>.

© 2013 Wiley-VCH Verlag & Co. KGaA, Boschstr. 12, 69469 Weinheim, Germany

All rights reserved (including those of translation into other languages). No part of this book may be reproduced in any form – by photoprinting, microfilm, or any other means – nor transmitted or translated into a machine language without written permission from the publishers. Registered names, trademarks, etc. used in this book, even when not specifically marked as such, are not to be considered unprotected by law.

Print ISBN: 978-3-527-33258-8

ePDF ISBN: 978-3-527-65115-3

ePub ISBN: 978-3-527-65114-6

mobi ISBN: 978-3-527-65113-9

oBook ISBN: 978-3-527-65112-2

Cover Design Formgeber, Eppelheim

Typesetting Laserwords Private Limited, Chennai, India

Printing and Binding Markono Print Media Pte Ltd, Singapore

Contents

Preface XIII

List of Contributors XV

1	Synthesis, Characterization, and Selected Properties of Graphene	1
	<i>C. N. R. Rao, Urmimala Maitra, and H. S. S. Ramakrishna Matte</i>	
1.1	Introduction	1
1.2	Synthesis of Single-Layer and Few-Layered Graphenes	4
1.2.1	Mechanical Exfoliation	5
1.2.2	Chemical Exfoliation	5
1.2.3	Chemical Vapor Deposition	8
1.2.4	Arc Discharge	8
1.2.5	Reduction of Graphite Oxide	10
1.3	Synthesis of Graphene Nanoribbons	12
1.4	Selected Properties	15
1.4.1	Magnetic Properties	15
1.4.2	Electrical Properties	19
1.4.2.1	Supercapacitors	22
1.4.2.2	Photovoltaics and Photodetectors	24
1.4.2.3	Field Emission and Blue Light Emission	25
1.4.3	Molecular Charge Transfer	25
1.4.4	Decoration with Metal and Oxide Nanoparticles	28
1.4.5	Surface Area and Gas Adsorption	30
1.4.6	Mechanical Properties	32
1.4.7	Quenching of Fluorescence of Aromatics	34
1.4.8	Chemical Storage of Hydrogen and Halogens	36
1.5	Inorganic Graphene Analogs	39
	References	40
2	Understanding Graphene via Raman Scattering	49
	<i>A. K. Sood and Biswanath Chakraborty</i>	
2.1	Introduction	49
2.2	Atomic Structure and Electronic Structure of Graphene	49
2.3	Phonons and Raman Modes in Graphene	51

2.4	Layer Dependence of Raman Spectra	57
2.4.1	G-Band	57
2.4.2	2D-Band	57
2.4.3	D-Band	59
2.4.4	Combination Modes in the Range 1650–2300 cm^{-1}	59
2.4.5	Low-Frequency Modes	61
2.5	Phonon Renormalization Due to Electron and Hole Doping of Graphene	61
2.5.1	Optical Phonon Mixing in Doped Bi- and Multilayer Graphene	66
2.5.2	Charge Inhomogeneity and p–n Junction in the FET Channel Probed by Raman Spectroscopy	68
2.6	Raman Spectroscopy of Graphene Edges and Graphene Nanoribbons	70
2.6.1	Effect of the Edge Orientation on the G-Band	70
2.6.2	Effect of the Edge Orientation on the D-Band	72
2.6.3	Raman Spectroscopy of Graphene Nanoribbons	73
2.7	Effect of Disorder on the Raman Spectrum of Graphene	74
2.8	Raman Spectroscopy of Graphene under Strain	77
2.9	Temperature and Pressure Dependence of Raman Modes in Graphene as Nanometrological Tools	83
2.10	Tip-Enhanced Raman Spectroscopy of Graphene Layers	85
2.11	Conclusions	86
	Acknowledgments	87
	References	87
3	Physics of Quanta and Quantum Fields in Graphene	91
	<i>Ganapathy Baskaran</i>	
3.1	Introduction	91
3.2	Dirac Theory in 3 + 1 Dimensions: A Review	93
3.3	Band Structure of Graphene: Massless Chiral Dirac Electrons in 2 + 1 Dimensions	95
3.3.1	Phase Vortices of Bloch States in k-Space	99
3.4	Anomaly – A Brief Introduction	100
3.4.1	Anomalous Commutator in (1 + 1) Dimensions	101
3.4.2	Axial Anomaly in (1 + 1), (3 + 1) Dimensions	102
3.5	Graphene and 2 + 1-Dimensional Parity Anomaly	105
3.6	Zitterbewegung	107
3.7	Klein Paradox	110
3.8	Relativistic-Type Effects and Vacuum Collapse in Graphene in Crossed Electric and Magnetic Fields	111
3.9	Prediction of Spin-1 Quanta from Resonating Valence Bond Correlations	116
3.10	Majorana Zero Mode from Two-Channel Kondo Effect in Graphene	120

- 3.11 Lattice Deformation as Gauge Fields 125
- 3.12 Summary 127
- Acknowledgment 127
- References 127

- 4 Magnetism of Nanographene 131**
- Toshiaki Enoki*
- 4.1 Introduction 131
- 4.2 Theoretical Background of Magnetism in Nanographene and Graphene Edges 134
- 4.3 Experimental Approach to Magnetism of Nanographene 139
- 4.3.1 Magnetic Structure of Edge-State Spins in Nanographene 139
- 4.3.2 Magnetism of σ -Dangling Bond Defects in Graphene 143
- 4.4 Magnetic Phenomena Arising in the Interaction with Guest Molecules in Nanographene-Based Nanoporous Carbon 146
- 4.4.1 Magnetic Switching Phenomenon 146
- 4.4.2 Helium Sensor 152
- 4.5 Summary 154
- Acknowledgment 155
- References 155

- 5 Physics of Electrical Noise in Graphene 159**
- Vidya Kochat, Srijit Goswami, Atindra Nath Pal, and Arindam Ghosh*
- 5.1 Introduction 159
- 5.1.1 Single-Layer Graphene 159
- 5.1.1.1 Effective Tight-Binding Hamiltonian: Sublattice and Valley Symmetry 161
- 5.1.1.2 Valley and Sublattice Pseudospin 161
- 5.1.1.3 Chirality 162
- 5.1.1.4 Berry Phase and Absence of Backscattering 162
- 5.1.2 Bilayer Graphene 163
- 5.1.2.1 Biased Bilayer Graphene 164
- 5.1.3 Multilayer Graphene 165
- 5.1.4 Disorder and Scattering Mechanism in Graphene 166
- 5.1.4.1 Coulomb Impurity Scattering 167
- 5.1.4.2 Phonon Scattering 169
- 5.1.4.3 Electron–Hole Puddles at Low Density 169
- 5.2 Flicker Noise or “ $1/f$ ” Noise in Electrical Conductivity of Graphene 169
- 5.2.1 Microscopic Origin of $1/f$ Noise in Graphene 173
- 5.2.2 Effect of Bandgap on Low-Frequency Noise in Bilayer Graphene 175
- 5.2.3 Shot Noise in Graphene 178
- 5.3 Noise in Quantum Transport in Graphene at Low Temperature 179
- 5.3.1 Quantum Transport in Mesoscopic Graphene 179
- 5.3.2 Universal Conductance Fluctuations in Graphene 184

5.4	Quantum-Confined Graphene	188
5.4.1	1D Graphene–Nanoribbons (GNRs)	188
5.5	Conclusions and Outlook	193
	References	193
6	Suspended Graphene Devices for Nanoelectromechanics and for the Study of Quantum Hall Effect	197
	<i>Vibhor Singh and Mandar M. Deshmukh</i>	
6.1	Introduction	197
6.2	Quantum Hall Effect in Graphene	198
6.3	Fabrication of Suspended Graphene Devices	200
6.4	Nanoelectromechanics Using Suspended Graphene Devices	201
6.5	Using Suspended Graphene NEMS Devices to Measure Thermal Expansion of Graphene	203
6.6	High-Mobility Suspended Graphene Devices to Study Quantum Hall Effect	206
	Acknowledgments	208
	References	208
7	Electronic and Magnetic Properties of Patterned Nanoribbons: A Detailed Computational Study	211
	<i>Biplab Sanyal</i>	
7.1	Introduction	211
7.2	Experimental Results	212
7.3	Theory of GNRs	214
7.3.1	Tight-Binding Method	214
7.3.2	First Principles Studies	217
7.4	Hydrogenation at the Edges	219
7.4.1	Stability of Nanoribbons	219
7.4.2	Dihydrogenated Edges	219
7.5	Novel Properties	226
7.6	Outlook	231
	Acknowledgements	231
	References	231
8	Stone–Wales Defects in Graphene and Related Two-Dimensional Nanomaterials	235
	<i>Sharmila N. Shirodkar and Umesh V. Waghmare</i>	
8.1	Introduction	235
8.2	Computational Methods	236
8.3	Graphene: Stone–Wales (SW) Defects	237
8.3.1	Structural, Electronic, Magnetic, and Vibrational Properties of Graphene with SW Defect	238
8.3.1.1	Structural Changes at an SW Defect	238
8.3.1.2	Interaction between SW Defects	239

8.3.1.3	Electronic Structure of Graphene and Effects of SW Defects	239
8.3.1.4	Magnetization due to Topological Defects	245
8.3.1.5	Effects on Vibrational Properties	246
8.3.2	Lattice Thermal Conductivity of Graphene with SW Defect	252
8.3.2.1	Theoretical Model	252
8.3.2.2	κ : Results	253
8.3.3	Discussion	254
8.4	$C_{1-x}(BN)_{x/2}$: C–BN Interfaces	255
8.4.1	SW Defect at the C–BN Interface	256
8.4.2	Discussion	259
8.5	Two-Dimensional MoS_2 and $MoSe_2$	259
8.5.1	Point Defects	259
8.5.2	Stacking Faults	261
8.5.3	IR Radiation Absorption	261
8.5.4	Discussion	265
8.6	Summary	265
	Acknowledgments	266
	References	266
9	Graphene and Graphene-Oxide-Based Materials for Electrochemical Energy Systems	269
	<i>Ganganahalli Kotturappa Ramesha and Srinivasan Sampath</i>	
9.1	Introduction	269
9.2	Graphene-Based Materials for Fuel Cells	270
9.2.1	Graphene-Based Catalyst Support for Small Molecule Redox Reactions	271
9.2.2	Graphene-Oxide-Based Proton Conducting Membranes	278
9.2.3	Graphene-Based Biofuel Cells	279
9.3	Graphene-Based Supercapacitors	280
9.4	Graphene in Batteries	289
9.5	Conclusions and Future Perspectives	296
	References	297
10	Heterogeneous Catalysis by Metal Nanoparticles Supported on Graphene	303
	<i>M. Samy El-Shall</i>	
10.1	Introduction	303
10.2	Synthesis of Graphene and Metal Nanoparticles Supported on Graphene	304
10.2.1	Chemically Converted Graphene by Microwave-Assisted Chemical Reduction of Graphene Oxide	304
10.2.1.1	Metal Nanoparticles Supported on Graphene by Microwave Synthesis	307

10.2.2	Laser-Converted Graphene by Laser Reduction of Graphene Oxide	308
10.2.2.1	Laser-Assisted Photoreduction of Graphene Oxide in Different Solvents	313
10.2.3	Photochemical Reduction of Metal Ions and Graphene Oxide	315
10.2.3.1	Photoreduction of Gold Ions and GO in Different Solvents	315
10.2.3.2	Photoreduction of Silver Ions and GO in Different Solvents	316
10.2.3.3	Mechanism of Photocatalytic Reduction	318
10.3	Pd/Graphene Heterogeneous Catalysts for Carbon–Carbon Cross-Coupling Reactions	319
10.3.1	Pd/Graphene Catalysts Prepared by Microwave-Assisted Chemical Reduction of GO	319
10.3.1.1	Catalytic Activity and Range of Utility	320
10.3.1.2	Catalyst Recyclability	322
10.3.2	Pd/PRGO Catalysts Prepared by Laser Partial Reduction of GO	323
10.3.2.1	Laser Synthesis of Pd Nanoparticles on Structural Defects in Graphene	323
10.3.2.2	Mechanism of Partial Reduction of GO and Defect Generation	325
10.3.2.3	Application of Pd/PRGO Nanocatalysts to Suzuki Reaction	326
10.3.2.4	Recyclability of the Pd/PRGO Nanocatalysts in Suzuki Reaction	328
10.3.2.5	Applications of the Pd/PRGO Catalyst A to Heck and Sonogashira Reactions	329
10.4	CO Oxidation by Transition-Metal/Metal-Oxide Nanoparticles Supported on Graphene	330
10.5	Conclusions and Outlook	334
	Acknowledgment	335
	References	335
11	Graphenes in Supramolecular Gels and in Biological Systems	339
	<i>Santanu Bhattacharya and Suman K. Samanta</i>	
11.1	Introduction	339
11.1.1	Overview of 2D-Nanomaterials	339
11.1.2	Overview of Physical Gels	339
11.1.3	Different Types of Graphenes, Their Preparation, Functionalization, and Gelation	340
11.2	Toward the Gelation of GO	341
11.2.1	Effect of pH on the Gelation of GO	342
11.2.2	Effect of the Dimension of GO toward Gelation	343
11.2.3	Cross-Linker (Small Molecule/Polymer)-Induced GO Gels	343
11.2.4	Cation-Induced GO Gels	345
11.2.5	Surfactant-Induced GO Gels	346
11.2.6	Ionic-Liquid-Induced GO Gels	347
11.2.7	Gelation of Hemoglobin by GO and Sensing	347

11.2.8	Gelation of DNA by GO with Dye-Absorption and Self-Healing Properties	348
11.2.9	Gelation-Assisted Isolation of Graphene from Graphene-GO Mixture	350
11.3	Polymer-Assisted Formation of Multifunctional Graphene Gels	350
11.3.1	Thermal and pH Regulated GO-Polymer Hydrogels	351
11.3.2	Gelation-Assisted Polymer Nanocomposites	351
11.3.3	Mechanical Properties of GO-Polymer Hydrogels	353
11.3.4	Electrical Properties of GO-Polymer Hydrogels	354
11.3.5	Multifunctional GO Hydrogels	354
11.3.6	Stimuli-Responsive Hydrogels and Their Applications	355
11.4	Graphene Aerogels	356
11.5	Hydrogel and Organogel as the Host for the Incorporation of Graphene	358
11.6	Biological Applications Involving Graphene	360
11.7	Conclusions and Future Directions	368
	References	370
12	Biomedical Applications of Graphene: Opportunities and Challenges	373
	<i>Manzoor Koyakutty, Abhilash Sasidharan, and Shantikumar Nair</i>	
12.1	Introduction	373
12.2	Summary of Physical and Chemical Properties of Graphene	374
12.2.1	Surface Chemistry (Biochemistry of Graphene)	374
12.2.1.1	Interaction of Graphene Surfaces with Biomolecules	374
12.3	Cellular Uptake, Biodistribution, and Clearance	376
12.3.1	Influence of Surface Chemistry on Uptake	376
12.3.2	Uptake of Graphene by Macrophages	377
12.4	Toxicity of Graphene	379
12.4.1	Macrophage Toxicity	380
12.4.2	Hemocompatibility	381
12.4.2.1	Hemolysis	381
12.4.2.2	Effect on Hemostasis: Platelet Activation and Aggregation	382
12.4.2.3	Effect on Plasma Coagulation	384
12.4.3	Inflammatory Response	384
12.4.3.1	Immune Cell Stimulation and Suppression	386
12.4.4	Toxicity Mechanisms	387
12.4.4.1	Intracellular ROS and Apoptosis in Macrophages	388
12.5	Mitigation of Toxicity by Surface Modifications	390
12.6	<i>In vivo</i> Toxicity	391
12.7	Potential Application Areas: Opportunities	395
12.7.1	Drug Delivery	395
12.7.2	Gene Delivery	397

12.7.3	Biosensing Using Graphene	399
12.7.4	Graphene for Cellular Imaging	401
12.7.5	Graphene for Tissue Engineering	402
12.7.6	Anticancer Therapy: Photothermal Ablation of Cancer	403
12.8	Conclusions	404
	References	405
	Index	409

Preface

Graphene is a fascinating subject of recent origin, its first isolation being made possible through micromechanical cleavage of a graphite crystal. Since its discovery, graphene has caused great sensation because of its unusual electronic properties, and scientists from all over the world have been working on the varied facets of graphene. Thus, there has been much effort to synthesize both single-layer and few-layer graphenes by a number of methods. A variety of properties and phenomena have been investigated, and many of the studies have been directed toward understanding the physical and chemical properties of graphene. Raman spectroscopy has been particularly useful in unraveling various aspects of graphene. A graphene field-effect transistor, a basic building block of nanodevices, is a single-element laboratory to study electron–phonon interactions using Raman scattering. The low-frequency electrical noise or the flicker noise in graphene devices defines the figure of merit of a device and has contrasting behavior for single- and bilayer-graphene devices. Magnetic properties have been of equal interest with the indication that graphene may be ferromagnetic at room temperature, exhibiting magnetoresistance. Graphene nanoribbons have attracted attention because of their unique electronic structure and properties. Graphene also provides a playground for exploring many quantum field related phenomena such as Klein tunneling, antilocalization, zitterbewegung, vacuum collapse by Lorenz boost and so on. Suspended graphene devices have been used to study nanoscale electromechanics and quantum Hall effect.

A variety of applications of graphene have come to the fore. Its use in supercapacitors and batteries has been explored. Other properties of graphene, which are noteworthy, are those that enable its use in nanoelectronics, field emission and catalysis. Biological aspects of graphene have been investigated by a number of workers, with emphasis on its toxicity and its possible use for drug delivery.

In this book, we have tried to cover many of the salient aspects of graphene, which are of current interest. Although the book mostly deals with graphene, we have included some material on graphene-like inorganic layered materials. It is possible, however, that some topics have been left out owing to constraints on the size of the book and possible errors in judgement. We trust that the

book will be useful to students, teachers, and practitioners, and serves as an introduction to those who want to take part in the exciting developments of this subject.

June 2012

C.N.R. Rao
A.K. Sood

List of Contributors

Ganapathy Baskaran

The Institute of Mathematical
Sciences
C.I.T. Campus
Chennai 600 113
Tamil Nadu
India

and

Perimeter Institute for
Theoretical Physics
31 Caroline Street North
Waterloo
Ontario
Canada N2L 2Y5

Santanu Bhattacharya

Indian Institute of Science
Department of Organic
Chemistry
Bangalore 560 012
Tala Marg
Karnataka
India

and

The Chemical Biology Unit
Jawaharlal Nehru Centre for
Advanced Scientific Research
Bangalore 560 064
Jakkur
Karnataka
India

Biswanath Chakraborty

Indian Institute of Science
Department of Physics
Bangalore 560012
Karnataka
India

Mandar M. Deshmukh

Tata Institute of Fundamental
Research
Department of Condensed Matter
Physics and Materials Science
Homi Bhabha Road
Mumbai 400005
India

M. Samy El-Shall

Virginia Commonwealth
University
Department of Chemistry
Richmond
VA 23284-2006
USA

and

King Abdulaziz University
Department of Chemistry
Jeddah 21589
Kingdom of Saudi Arabia

Toshiaki Enoki

Tokyo Institute of Technology
Department of Chemistry
Ookayama
Meguro-ku
Tokyo 152-8551
Japan

Arindam Ghosh

Indian Institute of Science
Department of Physics
C.V. Raman Avenue
Bangalore 560012
Karnataka
India

Srijit Goswami

Indian Institute of Science
Department of Physics
C.V. Raman Avenue
Bangalore 560012
Karnataka
India

Vidya Kochat

Indian Institute of Science
Department of Physics
C.V. Raman Avenue
Bangalore 560012
Karnataka
India

Manzoor Koyakutty

Amrita Vishwa Vidyapeetham
University
Amrita Centre for Nanosciences
and Molecular Medicine
Elamakkara
Kochi 682041
Kerala
India

Urmimala Maitra

Jawaharlal Nehru Centre for
Advanced Scientific Research
International Centre for Materials
Science
Chemistry and Physics of
Materials Unit, and CSIR Centre
of Excellence in Chemistry
Jakkur P.O.
Bangalore 560 064
Karnataka
India

H. S. S. Ramakrishna Matte

Jawaharlal Nehru Centre for
Advanced Scientific Research
International Centre for Materials
Science
Chemistry and Physics of
Materials Unit, and CSIR Centre
of Excellence in Chemistry
Jakkur P.O.
Bangalore 560 064
Karnataka
India

Shantikumar Nair

Amrita Vishwa Vidyapeetham
University
Amrita Centre for Nanosciences
and Molecular Medicine
Elamakkara
Kochi 682041
Kerala
India

Atindra Nath Pal

Indian Institute of Science
Department of Physics
C.V. Raman Avenue
Bangalore 560012
Karnataka
India

Ganganahalli Kotturappa**Ramesha**

Indian Institute of Science
Department of Inorganic and
Physical Chemistry
Bangalore 560 012
Karnataka
India

C. N. R. Rao

Jawaharlal Nehru Centre for
Advanced Scientific Research
International Centre for Materials
Science
Chemistry and Physics of
Materials Unit, and CSIR Centre
of Excellence in Chemistry
Jakkur P.O.
Bangalore 560 064
Karnataka
India

Suman K. Samanta

Indian Institute of Science
Department of Organic
Chemistry
Bangalore 560 012
Tala Marg
Karnataka
India

Srinivasan Sampath

Indian Institute of Science
Department of Inorganic and
Physical Chemistry
Bangalore 560 012
Karnataka
India

Biplab Sanyal

Uppsala University
Department of Physics and
Astronomy
Box-516
75120 Uppsala
Sweden

Sharmila N. Shirodkar

Theoretical Sciences Unit
Jawaharlal Nehru Centre for
Advanced Scientific Research
Srirampura Cross
Jakkur P.O.
Bangalore 560 064
Karnataka
India

Vibhor Singh

Tata Institute of Fundamental
Research
Department of Condensed Matter
Physics and Materials Science
Homi Bhabha Road
Mumbai 400005
India

A. K. Sood

Indian Institute of Science
Department of Physics
Bangalore 560012
Karnataka
India

Abhilash Sasidharan

Amrita Vishwa Vidyapeetham
University
Amrita Centre for Nanosciences
and Molecular Medicine
Elamakkara
Kochi 682041
Kerala
India

Umesh V. Waghmare

Theoretical Sciences Unit
Jawaharlal Nehru Centre for
Advanced Scientific Research
Srirampura Cross
Jakkur P.O.
Bangalore 560 064
Karnataka
India

1

Synthesis, Characterization, and Selected Properties of Graphene

C. N. R. Rao, Urmimala Maitra, and H. S. S. Ramakrishna Matte

1.1 Introduction

Carbon nanotubes (CNTs) and graphene are two of the most studied materials today. Two-dimensional graphene has specially attracted a lot of attention because of its unique electrical properties such as very high carrier mobility [1–4], the quantum Hall effect at room temperature [2, 5], and ambipolar electric field effect along with ballistic conduction of charge carriers [1]. Some other properties of graphene that are equally interesting include its unexpectedly high absorption of white light [6], high elasticity [7], unusual magnetic properties [8, 9], high surface area [10], gas adsorption [11], and charge-transfer interactions with molecules [12, 13]. We discuss some of these aspects in this chapter. While graphene normally refers to a single layer of sp^2 bonded carbon atoms, there are important investigations on bi- and few-layered graphenes (FGs) as well. In the very first experimental study on graphene by Novoselov *et al.* [1, 2] in 2004, graphene was prepared by micromechanical cleavage from graphite flakes. Since then, there has been much progress in the synthesis of graphene and a number of methods have been devised to prepare high-quality single-layer graphenes (SLGs) and FGs, some of which are described in this chapter.

Characterization of graphene forms an important part of graphene research and involves measurements based on various microscopic and spectroscopic techniques. Characterization involves determination of the number of layers and the purity of sample in terms of absence or presence of defects. Optical contrast of graphene layers on different substrates is the most simple and effective method for the identification of the number of layers. This method is based on the contrast arising from the interference of the reflected light beams at the air-to-graphene, graphene-to-dielectric, and (in the case of thin dielectric films) dielectric-to-substrate interfaces [14]. SLG, bilayer-, and multiple-layer graphenes (<10 layers) on Si substrate with a 285 nm SiO_2 are differentiated using contrast spectra, generated from the reflection light of a white-light source (Figure 1.1a) [15]. A total color difference (TCD) method, based on a combination of the reflection spectrum calculation and the International Commission on Illumination (CIE) color space

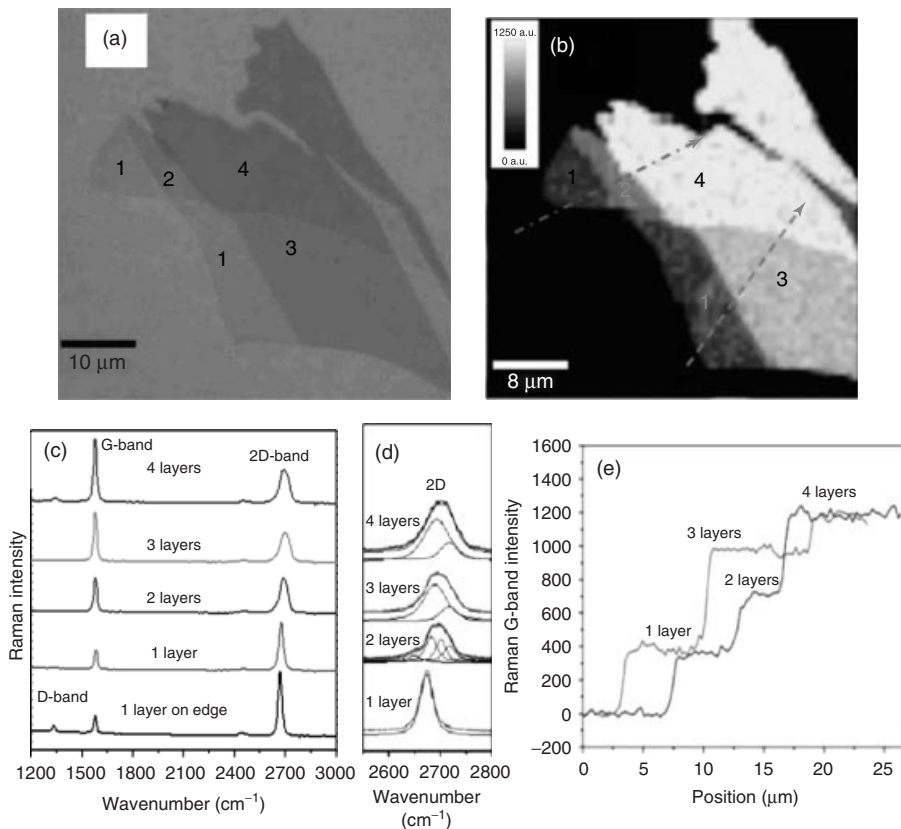


Figure 1.1 (a) Optical image of graphene with one, two, three, and four layers; (b) Raman image plotted by the intensity of G-band; (c) Raman spectra as a function of the number of layers; (d) zoom-in view

of the Raman 2D-band; and (e) the cross section of the Raman image, which corresponds to the dashed lines in (b). (Source: Reprinted with permission from Ref. [15].)

is also used to quantitatively investigate the effect of light source and substrate on the optical imaging of graphene for determining the thickness of the flakes. It is found that 72 nm thick Al_2O_3 film is much better at characterizing graphene than SiO_2 and Si_3N_4 films [16].

Contrast in scanning electron microscopic (SEM) images is another way to determine the number of layers. The secondary electron intensity from the sample operating at low electron acceleration voltage has a linear relationship with the number of graphene layers (Figure 1.2a) [17]. A quantitative estimation of the layer thicknesses is obtained using attenuated secondary electrons emitted from the substrate with an in-column low-energy electron detector [18]. Transmission electron microscopy (TEM) can be directly used to observe the number of layers on viewing the edges of the sample, each layers corresponding to a dark line. Gass *et al.* [19] observed individual atoms in graphene by high-angle annular

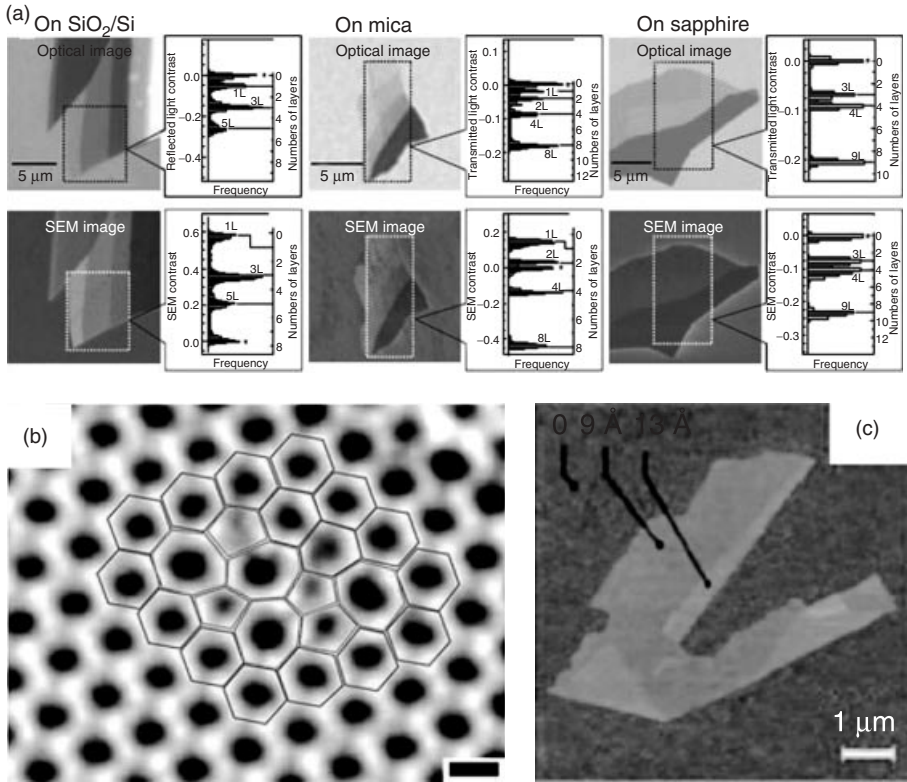


Figure 1.2 (a) Comparison of the counting of layers by optical microscopy and SEM for graphene on SiO₂/Si, mica, and sapphire. For each figure is shown a histogram of the distribution of graphene layers within the rectangular area indicated by a dotted line. (Source: Reprinted with permission from Ref. [17].) (b) High-resolution

transmission electron microscopic image showing the Stone–Wales defects in graphene. (Source: Reprinted with permission from Ref. [20].) (c) Atomic force microscopic image of single-layered graphene. Folded edge shows a height increase of 4 Å indicating single-layer graphene. (Source: Reprinted with permission from Ref. [3].)

dark-field (HAADF) scanning transmission electron microscopy (STEM) in the aberration-corrected mode at an operation voltage of 100 kV. Direct visualization of defects in the graphene lattice, such as the Stone–Wales defect, has been possible by aberration-corrected TEM with monochromator (Figure 1.2b) [20]. Electron diffraction can be used for differentiating the single layer from multiple layers of graphene. In SLG, there is only the zero-order Laue zone in the reciprocal space, and the intensities of diffraction peaks do not therefore, change much with the incidence angle. In contrast, bilayer graphene exhibits changes in total intensity with different incidence angles. Thus, the weak monotonic variation in diffraction intensities with tilt angle is a reliable way to identify monolayer graphene [21]. The relative intensities of the electron diffraction pattern from the {2110} and {1100} planes can be used to determine the number of layers. If $I_{\{1100\}}/I_{\{2110\}}$ is

>1 , it is reported as SLG, and if the ratio is <1 , it is multilayer graphene [22]. Thickness of graphene layers can be directly probed by atomic force microscopy (AFM) in tapping mode. On the basis of the interlayer distance in graphite of 3.5 \AA [3], the thickness of a graphene flake or the number of layers is determined as shown in Figure 1.2c [3]. Scanning tunneling microscopy (STM) also provides high-resolution images of graphene.

Raman spectroscopy has been extensively used as a nondestructive tool to probe the structural and electronic characteristics of graphene [3]. Figure 1.1c shows typical Raman spectra of one-, two-, three-, and four-layered graphene prepared using micromechanical cleavage technique and placed on SiO_2/Si substrate. The Raman spectrum of graphene has three major bands. The D-band located around 1300 cm^{-1} is a defect-induced band. The G-band located around 1580 cm^{-1} is due to in-plane vibrations of the sp^2 carbon atoms. The 2D-band around 2700 cm^{-1} results from a second-order process. The appearance of the D- and 2D-bands is related to the double resonance Raman scattering process [23], and with the increasing the number of layers, the 2D-band gets broadened and blue shifted. A sharp and symmetric 2D-band is found in the case of SLG as shown in Figure 1.1d. The Raman image obtained from the intensity of the G-band is shown in Figure 1.1b. A linear increase in the intensity profile of the G-band with increase in the number of layers along the dashed line is shown in Figure 1.1e [15]. Surface area, which also forms an important characteristic of graphene, is discussed later in the chapter.

1.2

Synthesis of Single-Layer and Few-Layered Graphenes

SLG and FG have been synthesized by several methods. In Table 1.1, we have listed some of these methods. The synthesis procedure can be broadly classified into exfoliation, chemical vapor deposition (CVD), arc discharge, and reduction of graphene oxide.

Table 1.1 Synthesis of single- and few-layered graphene.

Graphene synthesis	
Single layer	Few layers
Micromechanical cleavage of HOPG	Chemical reduction of exfoliated graphene oxide (2–6 layers)
CVD on metal surfaces	
Epitaxial growth on an insulator (SiC)	Thermal exfoliation of graphite oxide (2–7 layers)
Intercalation of graphite	Aerosol pyrolysis (2–40 layers)
Dispersion of graphite in water, NMP	
Reduction of single-layer graphene oxide	Arc discharge in presence of H_2 (2–4 layers)

1.2.1

Mechanical Exfoliation

Stacking of sheets in graphite is the result of overlap of partially filled p_z or π orbital perpendicular to the plane of the sheet (involving van der Waals forces). Exfoliation is the reverse of stacking; owing to the weak bonding and large lattice spacing in the perpendicular direction compared to the small lattice spacing and stronger bonding in the hexagonal lattice plane, it has been tempting to generate graphene sheets through exfoliation of graphite (EG). Graphene sheets of different thickness can indeed be obtained through mechanical exfoliation or by peeling off layers from graphitic materials such as highly ordered pyrolytic graphite (HOPG), single-crystal graphite, or natural graphite. Peeling and manipulation of graphene sheets have been achieved through AFM and STM tips [24–29]. Greater control over folding and unfolding could be achieved by modulating the distance or bias voltage between the tip and the sample [29]. Zhang [30] obtained 10–100 nm thick graphene sheets using graphite island attached to tip of micromachined Si cantilever to scan over SiO_2/Si surface. Folding and tearing of the sheets arise due to the formation of sp^3 -like line defects in the sp^2 graphitic network, occurring preferentially along the symmetry axes of graphite.

Novoselov *et al.* [1] pressed patterned HOPG square meshes on a photo resist spun over a glass substrate followed by repeated peeling using scotch tape and then released the flakes so obtained in acetone. Some flakes got deposited on the SiO_2/Si wafer when dipped in the acetone dispersion. Using this method, atomically thin graphene sheets were obtained. This method was simplified to just peeling off of one or a few sheets of graphene using scotch tape and depositing them on SiO_2 (300 nm)/Si substrates. Although mechanical exfoliation produces graphene of the highest quality (with least defects), the method is limited due to low productivity. Chemical exfoliation, on the other hand, possesses the advantages of bulk-scale production.

1.2.2

Chemical Exfoliation

Chemical exfoliation is a two-step process. The first step is to increase the interlayer spacing, thereby reducing the interlayer van der Waals forces. This is achieved by intercalating graphene to prepare graphene-intercalated compounds (GICs) [21]. The GICs are then exfoliated into graphene with single to few layers by rapid heating or sonication. A classic example of chemical exfoliation is the generation of single-layer graphene oxide (SGO) prepared from graphite oxide by ultrasonication [31–36]. Graphene oxide (GO) is readily prepared by the Hummers method involving the oxidation of graphite with strong oxidizing agents such as KMnO_4 and NaNO_3 in $\text{H}_2\text{SO}_4/\text{H}_3\text{PO}_4$ [31, 33]. On oxidation, the interlayer spacing increases from 3.7 to 9.5 Å, and exfoliation resulting in SLG is achieved by simple ultrasonication in a DMF/water (9 : 1) (dimethyl formamide) mixture. The SGO so prepared has a high density of functional groups, and reduction needs to be carried

out to obtain graphene-like properties. Chemical reduction has been achieved with hydrazine monohydrate to give well-dispersed SLG sheets [32, 35]. Thermal exfoliation and reduction of graphite oxide also produce good-quality graphene, generally referred to as reduced graphene oxide (RGO).

Rapid heating ($>200^\circ\text{C min}^{-1}$) to 1050°C also breaks up functionalized GO into individual sheets through evolution of CO_2 [37, 38]. A statistical analysis by AFM has shown that 80% of the observed flakes are single sheets [38]. Exfoliation of commercial expandable graphite has also been carried out by heating at 1000°C in forming gas for 60 s [39]. The resultant exfoliated graphite was reintercalated with oleum and tetrabutylammonium hydroxide (TBA). On sonication in a DMF solution of 1,2-distearoyl-*sn*-glycero-3-phosphoethanolamine-*N*-[methoxy-(polyethylene glycol)-5000] (DSPE-mPEG) for 60 min, the graphite-containing oleum and TBA get exfoliated to give a homogeneous suspension of SLG. These sheets can be made into large, transparent, conducting assembly in a layer-by-layer manner in organic solvents. On rapid heating, decomposition rate of the epoxy and hydroxyl groups of GO exceeds the diffusion rate of the evolved gases resulting in pressures that exceed the van der Waals forces holding the graphene sheets together and then exfoliation occurs. Exfoliated graphene sheets are highly wrinkled and have defects. As a result, these sheets do not collapse back to graphite but remain as highly agglomerated graphene sheets. Guoqing *et al.* [40] used microwaves to give thermal shock to acid-intercalated graphite oxide in order to carry out exfoliation. When irradiated in microwave oven, eddy currents are generated because of the stratified structure of GO, yielding high temperatures by Joule's heating. Decomposition and gasification of the intercalated acids in graphite leads to a sudden increase in interlayer spacing and thereby reduces van der Waals interaction. Further sonication yields SLG and FG sheets. Liang *et al.* [41] patterned FG on SiO_2/Si substrates using the electrostatic force of attraction between HOPG and the Si substrate. Laser exfoliation of HOPG has also been used to prepare FG, using a pulsed neodymium-doped yttrium aluminum garnet (Nd:YAG) laser [42]. The product depends on laser fluence, a fluence of $\sim 5.0 \text{ J cm}^{-2}$, yielding high-quality graphene with ultrathin morphology.

GICs can be prepared by the intercalation of alkali metal ions. Viculis *et al.* [43] prepared K-, Cs-, and NaK_2 -intercalated graphite by reacting alkali metals with acid-intercalated exfoliated graphite in Pyrex sealed tubes. GICs were treated with ethanol causing a vigorous reaction to yield exfoliated FG. A schematic representation of the reaction is presented in Figure 1.3a. Potassium-intercalated GICs are also prepared using the ternary potassium salt $\text{K}(\text{THF})_x\text{C}_{24}$, and they get readily exfoliated in *N*-methylpyrrolidone (NMP), yielding a dispersion of negatively charged SLG that can then be deposited onto any substrate [44].

Solution-phase EG in an organic solvent such as NMP results in high SLG yields [22]. In this case, the energy required to exfoliate graphene is balanced by the solvent-graphene interaction. Such solvent-graphene interactions are

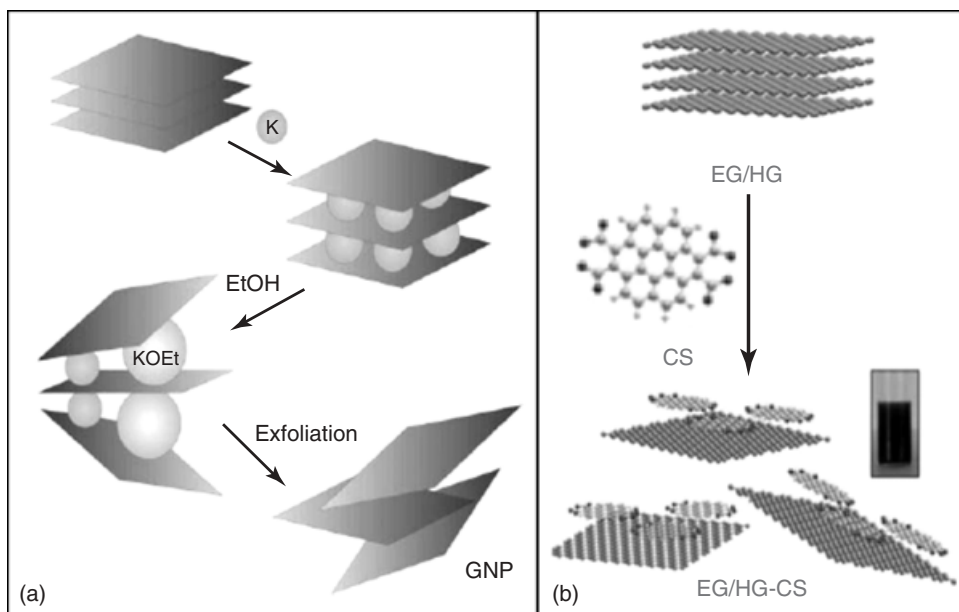


Figure 1.3 (a) Schematic diagram showing the intercalation of potassium between layers followed by violent reaction with alcohol to produce exfoliated ~ 30 layers of thin slabs of graphite. (Source: Reprinted with permission from Ref. [43].) (b) A schematic

illustration of the exfoliation of few-layer graphene with coronene tetracarboxylate (CS) to yield monolayer graphene–CS composites. (Source: Reprinted with permission from Ref. [45].)

also used to disperse graphene in perfluorinated aromatic solvents [46], orthodichloro benzene [47], and even in low-boiling solvents such as chloroform and isopropanol [48]. Hernandez *et al.* [49] carried out a detailed study on dispersibility of graphene in 40 different solvents and proposed that good solvents for graphene are characterized by the Hildebrand and Hansen solubility parameters. Greater than 63% of observed flakes had less than five layers in most solvents. Direct exfoliation and noncovalent functionalization and solubilization of graphene in water are achieved using the potassium salt of coronene tetracarboxylic acid (CS) to yield monolayer graphene–CS composites (Figure 1.3b) [45]. Stable high-concentration suspensions of FG were obtained by direct sonication in ionic liquids [50]. Exfoliation, reintercalation, and expansion of graphite yields highly conducting graphene sheets suspended in organic solvents [39]. Gram quantities of SLG have been produced from ethanol and sodium [51]. Under solvothermal conditions, alcoholic solutions of the metal get saturated with the metal alkoxide, and at autogenerated pressures of around 10^{-2} bar, the free alcohol gets encapsulated into the metal alkoxide in a clathrate-like structure. This is then pyrolyzed to yield a fused array of graphene sheets, and sonicated to yield SLG.

1.2.3

Chemical Vapor Deposition

The most promising, inexpensive, and readily accessible approach for the deposition of reasonably high quality graphene is CVD onto transition-metal substrates such as Ni [52], Pd [53], Ru [54], Ir [55], and Cu [56]. The process is based on the carbon saturation of a transition metal on exposure to a hydrocarbon gas at high temperature. While cooling the substrate, the solubility of carbon in the transition metal decreases and a thin film of carbon is thought to precipitate from the surface [57]. Different hydrocarbons such as methane, ethylene, acetylene, and benzene were decomposed on various transition-metal substrates such as Ni, Cu, Co, Au, and Ru [57].

A radio frequency plasma-enhanced chemical vapor deposition (PECVD) system has been used to synthesize graphene on a variety of substrates such as Si, W, Mo, Zr, Ti, Hf, Nb, Ta, Cr, 304 stainless steel, SiO₂, and Al₂O₃. This method reduces energy consumption and prevents the formation of amorphous carbon or other types of unwanted products [58–60]. Graphene layers have been deposited on different transition-metal substrates by decomposing hydrocarbons such as methane, ethylene, acetylene, and benzene. The number of layers varies with the hydrocarbon and reaction parameters. Nickel and cobalt foils that measure 5 × 5 mm² in area and 0.5 and 2 mm in thickness, respectively, have been used to carry out the CVD process at around 800–1000 °C; with nickel foil, CVD is carried out by passing methane (60–70 sccm) or ethylene (4–8 sccm) along with a high flow of hydrogen (around 500 sccm) at 1000 °C for 5–10 min. With benzene as the hydrocarbon source, benzene vapor diluted with argon and hydrogen was decomposed at 1000 °C for 5 min. On a cobalt foil, acetylene (4 sccm) and methane (65 sccm) were decomposed at 800 and 1000 °C, respectively. In all these experiments, the metal foils were cooled gradually after the decomposition. Figure 1.4 shows high-resolution TEM images of graphene sheets obtained by CVD on a nickel foil. Figure 1.4a shows graphenes obtained by the thermal decomposition of methane on the nickel foil, whereas Figure 1.4b shows graphene obtained by thermal decomposition of benzene. The insets in Figure 1.4a,b show selected area electron diffraction (SAED) patterns [61, 62]. All these graphene samples show G-band at 1580 cm⁻¹ and 2D band around 2670 cm⁻¹, with a narrow line width of 30–40 cm⁻¹. Figure 1.4c (i,ii) shows the Raman spectra of the graphene samples in Figure 1.4a,b, respectively. The narrow line width and relatively high intensity of the 2D-band confirm that these Raman spectra correspond to graphenes having one to two layers [57]. Graphene obtained by CVD process can be transferred to other substrates by etching the underlying transition metal and can be transformed into any arbitrary substrate.

1.2.4

Arc Discharge

Synthesis of graphene by the arc evaporation of graphite in the presence of hydrogen has been reported [61, 63]. This procedure yields graphene arc discharge graphene in H₂ atmosphere (HG) sheets with two to three layers having flake

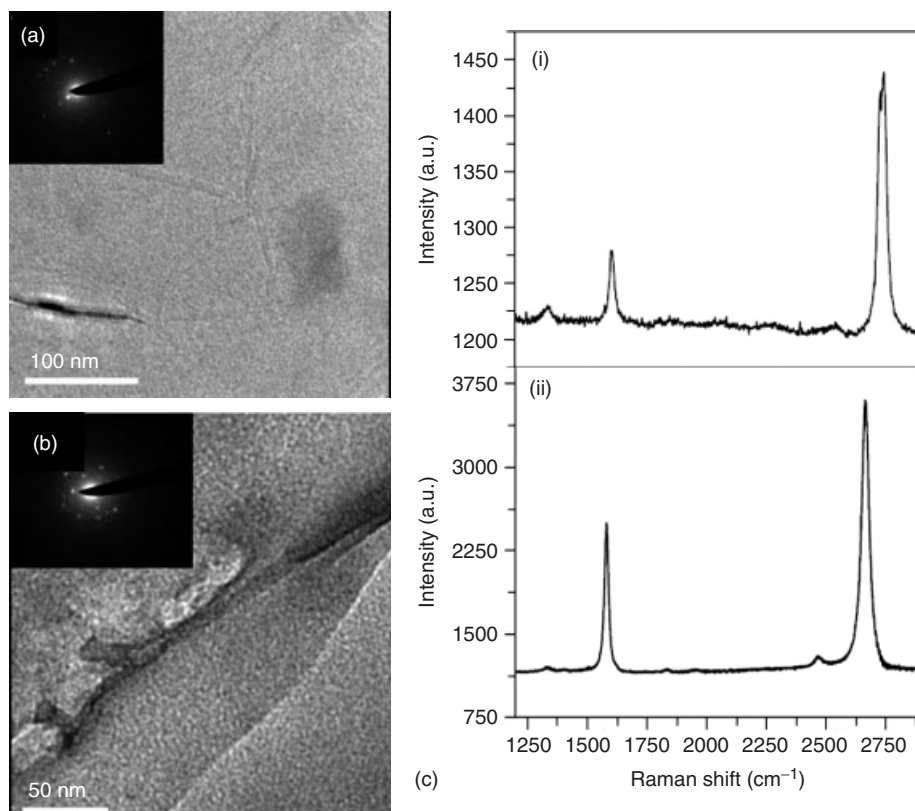


Figure 1.4 TEM images of graphene prepared by the thermal decomposition of (a) methane (70 sccm) at 1000 °C and (b) benzene (Ar passed through benzene with flow rate of 200 sccm) at 1000 °C on a nickel sheet. Insets show electron

diffraction pattern from the corresponding graphene sheets, and (c) the Raman spectra of graphene prepared from the thermal decomposition of (i) methane and (ii) benzene. (Source: Reprinted with permission from Ref. [61].)

size of 100–200 nm. This makes use of the knowledge that the presence of H_2 during arc discharge process terminates the dangling carbon bonds with hydrogen and prevents the formation of closed structures. The conditions that are favorable for obtaining graphene in the inner walls are high current (above 100 A), high voltage (>50 V), and high pressure of hydrogen (above 200 Torr). In Figure 1.5a,b, TEM and AFM images of HG sample are shown, respectively. This method has been conveniently used to dope graphene with boron and nitrogen [64]. To prepare boron-doped graphene (B-HG) and nitrogen-doped graphene (N-HG), the discharge is carried out in the presence of $H_2 +$ diborane and $H_2 +$ pyridine or ammonia, respectively. Later, based on these observations, some modifications in the synthetic conditions also yielded FG in bulk scale. Cheng *et al.* [65] used hydrogen arc discharge process as a rapid heating method to prepare graphene from GO. Arc discharge in an air atmosphere resulted in graphene nanosheets that

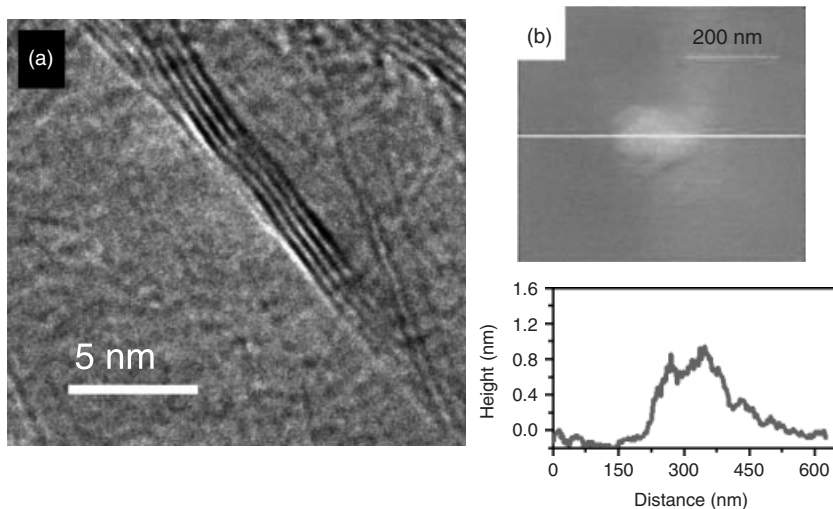


Figure 1.5 (a) TEM and (b) AFM image of HG prepared by arc discharge of graphite in hydrogen. Below is the height profile for the same. (Source: Reprinted with permission from Ref. [63].)

are ~ 100 – 200 nm wide predominantly with two layers. The yield depends strongly on the initial air pressure [66]. Li *et al.* [67] have synthesized N-doped multilayered graphene in He and NH_3 atmosphere using the arc discharge method. Arc discharge carried out in a helium atmosphere has been explored to obtain graphene sheets with different number of layers by regulating gas pressures and currents [68].

1.2.5

Reduction of Graphite Oxide

Chemical reduction of graphite oxide is one of the established procedures to prepare graphene in large quantities [33]. Graphite oxide when ultrasonicated in water forms a homogeneous colloidal dispersion of predominantly SGO in water. RGO with properties similar to that of graphene is prepared through chemical, thermal, or electrochemical reduction pathways [69]. While most strong reductants have slight to strong reactivity with water, hydrazine monohydrate does not, making it an attractive option for reducing aqueous dispersions of graphene oxide [70]. Syn addition of H_2 occurs across the alkenes, coupled with the extrusion of nitrogen gas. Large excess of NaBH_4 has also been used as a reducing agent [71]. Other reducing agents used include phenyl hydrazine [72], hydroxylamine [73], glucose [74], ascorbic acid [75], hydroquinone [76], alkaline solutions [77], and pyrrole [78]. Electrochemical reduction is another means to synthesize graphene in large scale [79–81]. The reduction initiates at -0.8 V and is completed by -1.5 V, with the formation of black precipitate onto the bare graphite electrode. Zhou *et al.* [82] coupled electrochemical reduction with a spray coating technique to prepare large-area and patterned RGO films with thicknesses ranging from a single